Int. Journal of Refractory Metals and Hard Materials 31 (2012) 288–292

Contents lists available at SciVerse ScienceDirect

Int. Journal of Refractory Metals and Hard Materials

journal homepage: www.elsevier.com/locate/IJRMHM

Short communication

Magnesium-assisted formation of metal carbides and nitrides from metal oxides

Liangbiao Wang, Qianwen Li, Yongchun Zhu *, Yitai Qian *

Hefei National Laboratory for Physical Science at Microscale and Department of Chemistry, University of Science and Technology of China, Hefei, Anhui 230026, People's Republic of China

ARTICLE INFO

Article history:
Received 13 August 2011
Accepted 22 October 2011

Keywords:
Carbides
Nitrides
Solid state reaction
X-ray diffraction

ABSTRACT

A series of carbides (TiC, V_2C, Mo_2C) were synthesized by the corresponding metal oxides (TiO_2, V_2O_5, MoO_3), CaC_2 and magnesium as starting materials in a stainless steel autoclave at 600 °C. Through similar processes, transition metal nitrides (TiN, VN and CrN) could also be produced by employing the corresponding metal oxides (TiO_2, V_2O_5, Cr_2O_3), $NaNH_2$, and magnesium as starting materials at 550 °C. The FE-SEM image showed that the TiC sample was mainly consisted of flower-like microstructures. TEM image showed the other carbides (V2C, Mo2C) and the obtained nitride (TiN, VN, CrN) were consisted of nanoparticles. The possible synthesis mechanism of TiC had been described.

1. Introduction

Metal carbides and nitrides have a wide range of applications in many fields due to their superior properties such as high melting point, extreme hardness, and high resistance to oxidation and corrosion [1,2]. For example, titanium carbide can be used as cutting tools and reinforcing components in composites [3]. Vanadium carbide is proved to be an active ammonia decomposition catalyst [4]. Molybdenum carbide is a powerful catalyst and considered as the potential substitute of noble metal in catalysis [5]. Titanium nitride can be used not only as abrasion resistant coatings but also as a catalyst for the alkylation of ketones with alcohols [6]. Vanadium nitride is a hard refractory material and used as electrodes in supercapacitors [7]. Chromium nitride can be used to coat steels for corrosion protection [8].

Traditionally, metal carbides and nitrides have been successfully synthesized by direct carbonation/nitridation of the elements (650–1900 °C) [9,10]; carbonation/nitridation of the metal oxides at high-temperature (>800 °C) [11,12]; thermal decomposition of precursors at relatively low temperature [13–15]; solid state metathesis (SSM) [16–18]; chemical vapor deposition (650–1200 °C) [19,20]; solvothermal synthesis [21–23]. The ball milling can be also used to synthesize transition metal carbides [24]. Nitrides can be prepared by ammonolysis of binary metal chlorides (>550 °C) [25], or metal sulfides (800 °C) [26]. Metal carbides and nitrides can be obtained by a soft urea pathway using urea as carbon/nitrogen source at 800 °C [27].

In this study, a magnesium-assisted approach was applied to synthesize transition metal carbides and nitrides. A series of carbides and nitrides were prepared from the corresponding metal oxides *via* a magnesium-assisted solid-state reaction. The reactions *via* the route can be indicated as:

$$2M_xO_y + CaC_2 + (2y-1)Mg = (2y-1)MgO + CaO + 2\ M_xC (M = Ti, V, Mo)$$

$$M_xO_y + x\ NaNH_2 + 2y\ Mg = 2y\ MgO + x\ Na + x\ H_2 + x\ MN\ (M = Ti,\ V,\ Cr)$$

2. Experimental procedure

2.1. Preparation of metal carbides

All chemical reagents used in this experiment were of analytical grade and used without further purification. In a typical synthesis process, transition metal oxides (2 mmol of TiO_2, 1 mmol of V_2O_5 or 2 mmol of MoO_3), 1 mmol of calcium carbide and 50 mmol of metallic magnesium were mixed in an agate mortar. The mixture was sealed in a stainless steel autoclave (20 mL). The temperature of the electronic furnace was raised from room temperature to 600 °C with a heating ramp rate of 10 °C/min and kept at 600 °C for 10 h, and then it was cooled to room temperature naturally. A dark precipitate was collected and washed with dilute hydrochloric acid under ultrasonic, absolute ethanol, and distilled water. The final product was dried in vacuum at 60 °C for 5 h.

2.2. Preparation of metal nitrides

In a typical synthesis process, metal oxides (2 mmol of TiO_2, 1 mmol of V_2O_5, or 1 mmol of Cr_2O_3), 0.1 mol of sodium amide and an excess of 20 mmol of metallic magnesuim were mixed and placed in a stainless-steel autoclave of 20 mL capacity. The autoclave was sealed and put into an electronic furnace which was heated from room temperature at 10 °C/min to 550 °C and then maintained for 10 h. After that, the

* Corresponding authors. Tel.: +86 551 360 1589; fax: +86 551 360 7402.
E-mail address: wlb6641@163.com (Y. Qian).

0263-4368/$ – see front matter © 2011 Elsevier Ltd. All rights reserved.
doi:10.1016/j.ijrmhm.2011.10.009

autoclave was cooled to room temperature naturally. In order to remove the byproducts, the precipitates in the autoclave were collected and washed with dilute hydrochloric acid, absolute ethanol, and distilled water several times. After that, the products were dried in vacuum at 60 °C for 5 h for further characterization.

2.3. Characterization

Powder X-ray diffraction (XRD) measurements were carried out with a Philips X'pert X-ray diffractometer (CuKα λ = 1.54178 Å). X-Ray photoelectron spectra (XPS) were recorded on a VGESCALAB MKII X-ray photoelectron spectrometer, using non-monochromated Mg Kα X-ray radiation as the excitation source. The scanning electron microscopy (SEM) images were taken by using a field-emitting scanning electron microscope (FESEM, JEOL-JSM-6700F). The transmission electron microscopy (TEM) images, high-resolution transmission electron microscopy (HRTEM) images and the selected-area electron diffraction (SAED) patterns were taken on a JEOL-2010 transmission electron microscope with an accelerating voltage of 200 kV.

3. Results and discussion

3.1. Characterization of the synthesized TiC

X-Ray powder diffraction (XRD) analysis was used to determine the phases of the samples. Fig. 1a shows the typical XRD pattern of the TiC sample. All of the peaks could be indexed to cubic TiC with lattice constant of $a = 4.3256$ Å, which is close to the value of cubic TiC ($a = 4.3276$ Å) (Joint Committee on Powder Diffraction Standards (JCPDS) card no. 73–0472). No other crystalline impurities were detected by XRD, which indicated the pure cubic TiC sample was obtained via the present synthetic route. FE-SEM, TEM, and HRTEM images of the TiC sample are shown in Fig. 1b–d. The FE-SEM image in Fig. 1b shows that the sample is mainly consisted of flower-like microstructures together with a small fraction of the irregular particles. The diameter of microstructures ranges from 0.5 to 1 μm. The FE-SEM image indicates that the flower-like microstructures are composed of nanosheets. The microstructure of the sample was further determined with TEM, which prove the result of the FE-SEM (was shown in Fig. 1c). Moreover, the selected area electron diffraction pattern (inset of Fig. 1c) can be indexed to the 111 and 200 reflections in cubic TiC consistent with the crystal viewed down the $[01\bar{1}]$ axis. The HRTEM image of a nanosheet shown in Fig. 1d presents the lattice spacing. The distance separating the lattice fringes, around 0.25 nm, coincides with the distance between two (111) planes in cubic TiC.

The XPS spectrum of as-prepared TiC was also investigated (Fig. 2). As can be seen from the curve a and b,, three strong peaks centered at about 281.50, 454.71, and 460.68 eV correspond to the C1s, Ti2p3/2, and Ti2p1/2 binding energy of TiC in literature [28]. An average composition of Ti: C is 1.12: 1 which could be quantified by the Ti2p and C1s peak areas.

3.2. Characterization of the synthesized V_2C and Mo_2C

The XRD patterns of V_2C (upper in Fig. 3a) and Mo_2C (bottom in Fig. 3a) samples were shown in the Fig. 3a. The sharp peaks with strong diffraction intensity in the Fig. 3a can be appropriately indexed to hexagonal V_2C (JCPDS card no. 73-1320) and hexagonal Mo_2C (JCPDS card no. 35-0787). The TEM image of V_2C sample (Fig. 3b) reveals the sample is composed of nanoparticles with the average size of 50 nm. The SAED rings (upper-right in Fig. 3b) correspond to (100), (002), (101), (102), and (110) planes of the hexagonal V_2C, which consists with the XRD results. The HRTEM image of V_2C (bottom-right in Fig. 3b) clearly exhibits the lattice fringe spacing for (100) plane of hexagonal V_2C ($d_{100} = 0.251$ nm), which further proves that V_2C was prepared. The TEM image of the as-prepared nanocrystalline Mo_2C is shown in Fig. 3c. The average size of the primary particles is 30 nm. The SAED rings shown in the inset of Fig. 3c are consistent with the XRD pattern of Mo_2C. Fig. 3d is a HRTEM image of Mo_2C. The regular spacing of the lattice planes is 0.26 nm, which is in agreement with (100) plane of the Mo_2C.

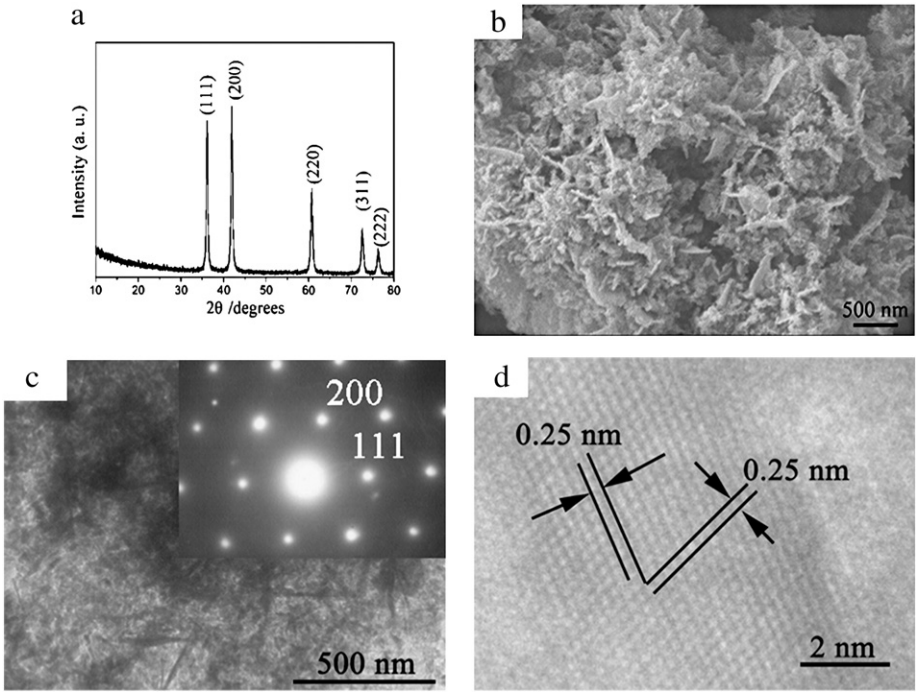

Fig. 1. (a) XRD patterns of as-prepared TiC, (b) FE-SEM pattern of as-prepared TiC; (c) TEM of the as-prepared TiC. The inset shows the corresponding SAED patterns; (d) HRTEM image of the as-prepared TiC.

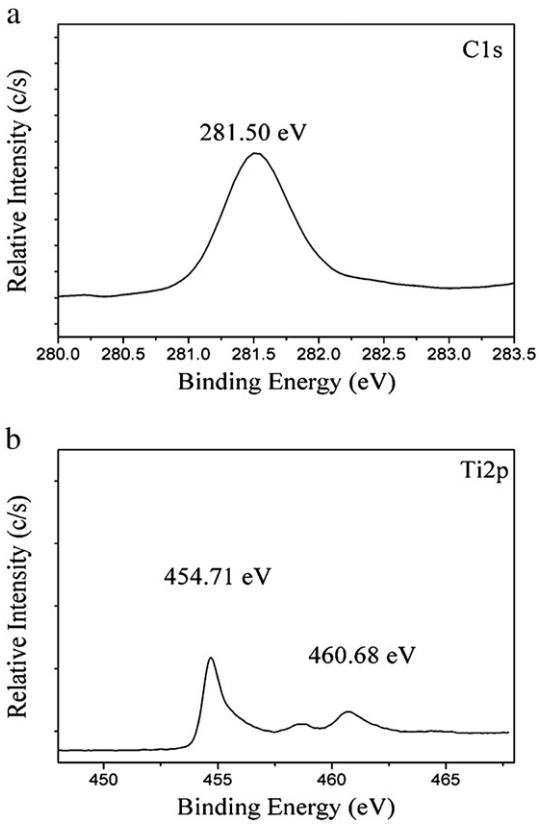

Fig. 2. XPS spectra of the as-prepared TiC (a) C1s region, (b) Ti2p region.

3.3. Characterization of the synthesized TiN, VN and CrN

Transition metal oxides such as TiO_2, V_2O_5, and Cr_2O_3 can be converted into related nitrides by this route at 550 °C. X-ray diffraction was used to verify the crystal structures and the phase purity of the materials. The XRD pattern of the synthesized TiN was shown in Fig. 4a. The XRD pattern indicates that the synthesized TiN has a NaCl-type structure with lattice constant of $a = 4.240$ Å, consistent with the reported value of cubic TiN (JCPDS card, No. 38-1420 $a = 4.241$ Å). No other peaks of impurities of metals or metal oxides can be found from the patterns. The morphologies of the prepared samples were investigated by TEM. The TEM image of the TiN is shown in Fig. 4b, which indicates the synthesized TiN consists of particles in the range of 20–30 nm in diameter. Moreover, the SAED rings/spots (inset of Fig. 4b,) correspond to the (111), (200), and (220) planes of TiN, which confirm the XRD result. The XRD pattern of the synthesized VN nanocrystals was shown in Fig. 5a. All the strong peaks can be indexed to the NaCl-type structure of VN with lattice parameter $a = 4.137$ Å, which is in good agreement with the reported value $a = 4.139$ Å ((JCPDS) card, No. 35-0768). The TEM image of the synthesized VN (Fig. 5b) shows that the size of the nanocrystals is in the range of 20–40 nm. Moreover, the SAED rings/spots (inset of Fig. 5b) can be indexed to the (111), (200), and (220) planes of cubic VN. The XRD pattern of the synthesized CrN nanocystals, shown in Fig. 6a, is basically the same as that of the cubic CrN phase (JCPDS card, No. 76-2494). The lattice constant calculated from the pattern ($a = 4.120$) is very close to the reported value for CrN ($a = 4.140$). TEM image of the synthesized CrN nanocrystals was shown in Fig. 6b, which shows that the particles are agglomerated, and have an average size of about 40 nm. The SAED rings/spots (inset of Fig. 6b) from inner to outer can be indexed to (111), (200) and (220) planes of cubic CrN, which are consistent with the XRD result.

3.4. The possible formation mechanism of the carbides– taking TiC as an example

The solid state metathesis (SSM) route is an effective method in generating metal carbides and nitrides by using metal halides or metal oxides as the metal sources. The process has the advantages of the relatively low reaction temperature and easy removal of the co-produced salt with water. Furthermore, the metal oxides are inexpensive and easy operation metal source in the SSM route, while it requires higher temperature (600–1200 °C) due to the high kinetic barriers. As we know, solid state metathesis reactions are driven

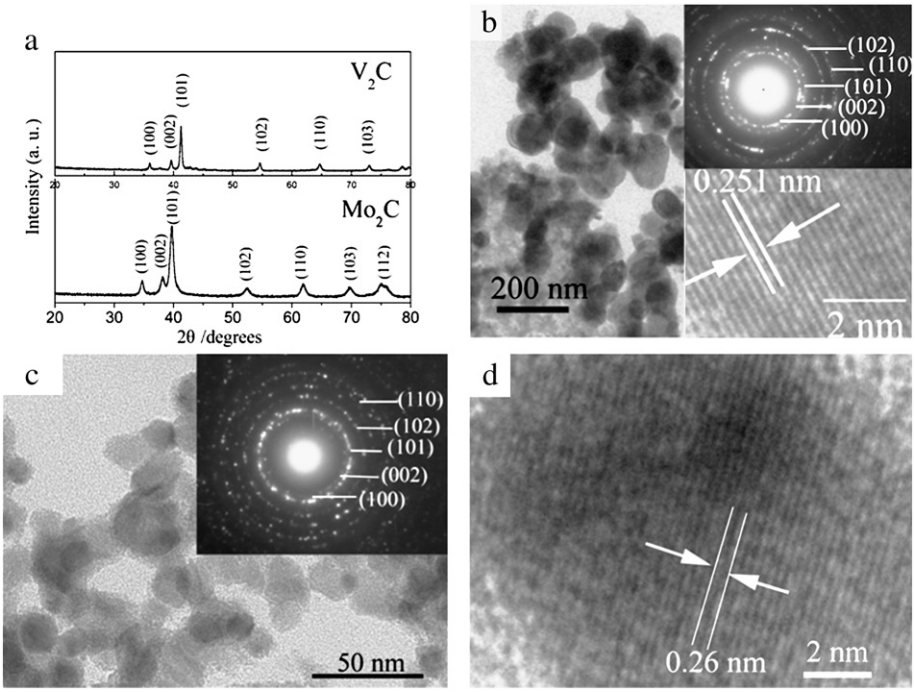

Fig. 3. (a) XRD patterns V_2C sample and Mo_2C sample; (b) TEM image of the as-prepared V2C sample, the inset shows the corresponding SAED patterns and HRTEM image; (c) TEM image of the as-prepared Mo_2C sample, the inset shows the corresponding SAED patterns; (d) HRTEM image of the as-prepared Mo_2C sample.

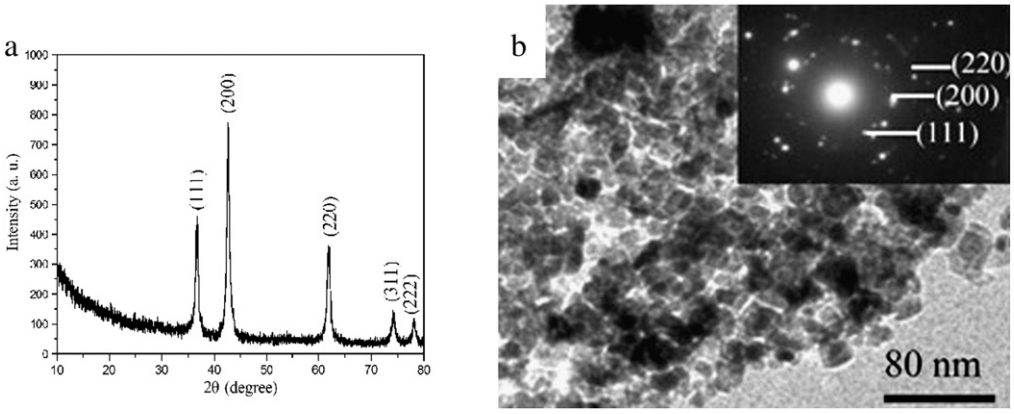

Fig. 4. (a) XRD pattern of the synthesized TiN; (b) TEM images of the synthesized TiN.

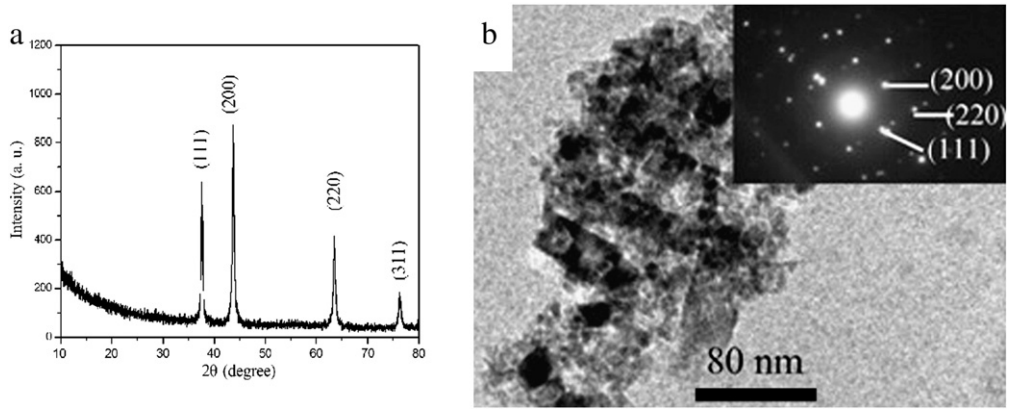

Fig. 5. (a) XRD pattern of the synthesized VN; (b) TEM images of the synthesized VN.

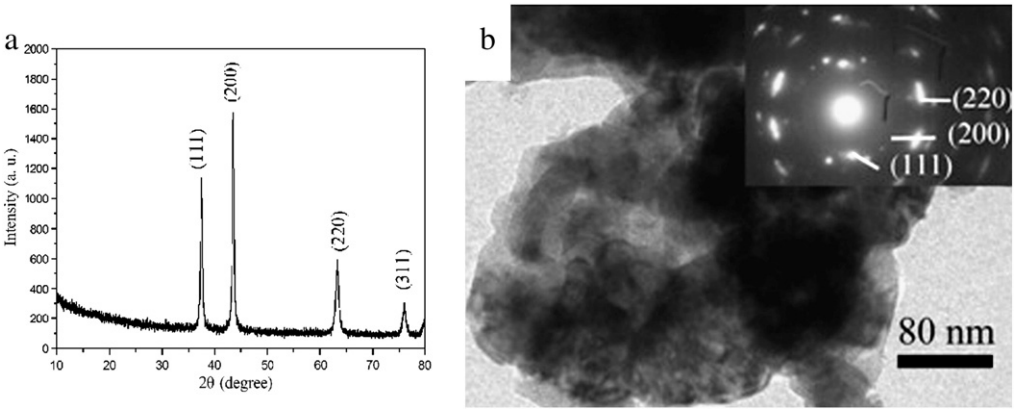

Fig. 6. (a) XRD pattern of the synthesized CrN; (b) TEM images of the synthesized CrN.

primarily by the lattice energy of the coproduced product. The large amount of heat generated in the solid state metathesis reaction urges the reaction to proceed continuously. A range of transition metal carbides were synthesized by the reaction of transition metal oxides with calcium carbide at 1000 °C for 12 h [29]. However, in the present work, we can produce the carbides from metal oxides and calcium carbide with magnesium-assisted at 600 °C. The experimental parameters such as reaction temperature, reactants, and time were investigated to determine the formation mechanism. Taking the formation of TiC as an example, titanium carbide can't be obtained when the temperature was set below 550 °C, while the carbides with good crystallinity were obtained at 600 °C. Under the present experimental conditions, it was found that only gray powder was obtained by the reaction of TiO_2 and CaC_2. The XRD pattern of the gray powder (Fig. 7a) can be indexed to TiO_2, which indicates that there is no reaction between TiO_2 and CaC_2 at 600 °C. To further understand the formation mechanism of the TiC, a series of time-dependence experiments were carried out. Fig. 7b, c and d show the XRD patterns of the products obtained by the reaction of CaC_2, Mg and TiO_2 for 30 min, 2 h and 4 h, respectively. The XRD patterns (Fig. 7b) can be indexed to the Ti_2O_3 (JCPDS card, No 85-0868), which shows that TiO_2 is reduced to form Ti_2O_3 by magnesium and no carbide (TiC) can be obtained within 30 min. The XRD patterns (Fig. 7c) can be indexed to the mixture of Ti_2O_3 and TiC because

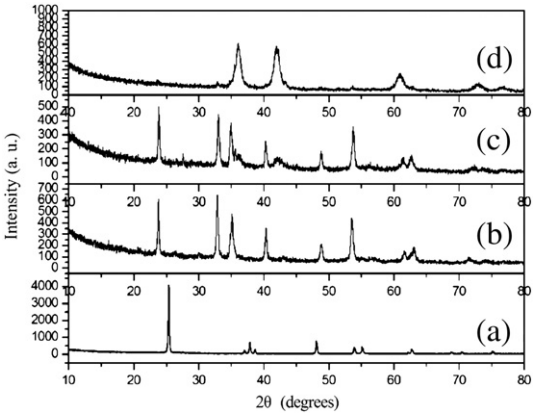

Fig. 7. (a) The XRD pattern of product obtained in the reaction between the CaC_2 and TiO_2. The XRD pattern of product obtained in the reaction between the CaC_2, Mg and TiO_2 with different heating time: (b) 30 min, (c) 2 h, and (d) 4 h.

several broad peaks can be indexed to cubic TiC except that of Ti_2O_3. This result indicates that TiC has been started to form. When the reaction time was prolonged to 4 h, the diffraction peaks of TiC were found in the XRD pattern (shown in Fig. 7d). From the Fig. 7d, the diffraction peaks of Ti_2O_3 can also be found coexisted with those of TiC. The diffraction peaks of the synthesized TiC were very broad in the XRD pattern (shown in Fig. 7d), which indicates that sizes of the obtained TiC are very small. As the reaction time extends from 4 to 10 h, the diffraction peaks in the XRD pattern (Fig. 1a) turn sharper. Based on the above-mentioned experimental facts, the synthesis mechanism has been described by follow processes: Firstly, TiO_2 was reduced to Ti_2O_3, which is similar to the literature [30]; then, TiC was obtained by the reaction Ti_2O_3, Mg and CaC_2. Therefore, the possible reaction could be expressed as follows,

$$2\,TiO_2 + Mg = MgO + Ti_2O_3$$

$$Ti_2O_3 + CaC_2 + 2\,Mg = 2\,MgO + CaO + 2\,TiC$$

However, the detailed formation mechanism of the metal carbides is also not clear, and the further experiment is underway.

4. Conclusion

Herein, through the magnesium-assisted solid-state reaction, we have successfully prepared metal carbides (TiC, V_2C, Mo_2C) and metal nitrides (TiN, VN, CrN) starting from the corresponding transition metal oxides at 550–600 °C. The FE-SEM image showed that the TiC sample is mainly consisted of flower-like microstructures. TEM image showed the other carbides (V_2C, Mo_2C) and the obtained nitride (TiN, VN, CrN) were consisted of nanoparticles. The possible synthesis mechanism of TiC had been described. This general and simple route may provide new insights into the synthesis of other metal carbides and nitrides.

Acknowledgements

The financial support of this work, by the 973 Project of China (No. 2011CB935901), is gratefully acknowledged.

References

[1] Hwu HH, Chen JGG. Surface chemistry of transition metal carbides. Chem Rev 2005;105(1):185–212.
[2] Niewa R, DiSalvo FJ. Recent developments in nitride chemistry. Chem Mater 1998;10:2733–52.
[3] Strzeciwilk D, Wokulski Z, Tkacz P. Microstructure of TiC crystals obtained from high temperature nickel solution. J Alloys Compd 2003;350(1–2):256–63.
[4] Choi JG. Ammonia decomposition over vanadium carbide catalysts. J Catal 1999;182(1):104–16.
[5] Solymosi F, Szoke A, Cserenyi J. Conversion of methane to benzene over Mo_2C and Mo2C/ZSM-5 catalysts. Catal Lett 1996;39(3–4):157–61.
[6] Fischer A, Makowski P, Mueller JO. High-surface-area TiO_2 and TiN as catalysts for the C–C coupling of alcohols and ketones. ChemSusChem 2008;1(5):444–9.
[7] Dong SM, Chen X, Gu L. TiN/VN composites with core/shell structure for supercapacitors. Mater Res Bull 2011;46(6):835–9.
[8] Su YL, Yao SH, Leu ZL. Comparison of tribological behavior of three films – TiN, TiCN and CrN – grown by physical vapor deposition. Wear 1997;213(1–2):165–74.
[9] Halverson DC, Ewald KH, Munir ZA. Influence of reactant characteristics on the microstructures of combustion-synthesized titanium carbide. J Mater Sci 1993;28(17):4583–94.
[10] Chen XZ, Dye JL, Eick HA. Synthesis of transition-metal nitrides from nanoscale metal particles prepared by homogeneous reduction of metal halides with an alkalide. Chem Mater 1997;9(5):1172–6.
[11] Koc R, Folmer JS. Carbothermal synthesis of titanium carbide using ultrafine titania powders. J Mater Sci 1997;32(12):3101–11.
[12] Chaudhury S, Mukerjee SK, Vaidya VN, Venugopal V. Kinetics and mechanism of carbothermic reduction of MoO_3 to Mo_2C. J Alloys Compd 1997;261(1–2):105–13.
[13] Jiang ZP, Rhine WE. Preparation of TiN and TiC from a polymeric precursor. Chem Mater 1991;3:1132–7.
[14] Giraudon JM, Leclercq L, Leclercq G, Lofberg A, Frennet A. Organometallic route to dimolybdenum carbide via a low-temperature pyrolysis of a dimolybdenum alkyne complex. J Mater Sci 1993;28:2449–54.
[15] Derraz Y, Cyrathis O, Choukroun R, Valade V, Cassoux P, Dahan F. *tert*-Butyl-substituted vanadocene, $(C_5H_4CMe_3)_2V$: a precursor for MOCVD of pure vanadium carbide. J Mater Chem 1995;5(11):1775–8.
[16] Nartowski AM, Parkin IP, MacKenzie M, Craven AJ, MacLeod I. Solid state metathesis routes to transition metal carbides. J Mater Chem 1999;9(6):1275–81.
[17] Song B, Jian JK, Wang G. Facile and general route to nitrides by a modified solid-state metathesis pathway. Chem Mater 2007;19(6):1497–502.
[18] Zhao HZ, Lei M, Yang X, Jian JK, Chen XL. Route to GaN and VN assisted by carbothermal reduction process. J Am Chem Soc 2005;127:15722–3.
[19] Lu J, Hugosson H, Eriksson O, Nordstrom L, Jansson U. Chemical vapour deposition of molybdenum carbides: aspects of phase stability. Thin Solid Films 2000;370(1–2):203–12.
[20] Qi SR, Huang XT, Gan ZW, Ding XX, Cheng Y. Synthesis of titanium carbide nanowires. J Cryst Growth 2000;219(4):485–8.
[21] Xie Y, Qian YT, Wang WZ. A benzene-thermal synthetic route to nanocrystalline GaN. Science 1996;272:1926–7.
[22] Gu YL, Guo F, Qian YT. A benzene-thermal synthesis of powdered cubic zirconium nitride. Mater Lett 2003;57(11):1679–82.
[23] Gu YL, Li ZF, Chen LY, Ying YC, Qian YT. Synthesis of nanocrystalline Mo_2C via sodium co-reduction of $MoCl_5$ and CBr_4 in benzene. Mater Res Bull 2003;38(7):1119–22.
[24] Xia ZP, Shen YQ, Shen JJ, Li ZQ. Mechanosynthesis of molybdenum carbides by ball milling at room temperature. J Alloys Compd 2008;453:185–90.
[25] Zhang ZD, Liu RM, Qian YT. Synthesis of nanocrystalline chromium nitride from ammonolysis of chromium chloride. Mater Res Bull 2002;37:1005–10.
[26] Herle PS, Hegde MS, Vasathacharya NY, Philip Sam. Synthesis of TiN, VN, and CrN from ammonolysis of TiS_2, VS_2, and Cr_2S_3. J Solid State Chem 1997;134:120–7.
[27] Giordano C, Erpen C, Yao WT, Antonietti M. Synthesis of Mo and W carbide and nitride nanoparticles via a simple "urea glass" route. Nano Lett 2008;8(12):4659–63.
[28] Galuska AA, Uht JC, Marquez N. Reactive and nonreactive ion mixing of Ni films on carbon substrates. J Vac Sci Technol A 1988;6(1):110–22.
[29] Nartowski AM, Parkin IP, MacKenzie M, Craven AJ. Solid state metathesis: synthesis of metal carbides from metal oxides. J Mater Chem 2001;11:3116–9.
[30] Sarkar D, Chu MC, Cho SJ, Kim YI. Synthesis and morphological analysis of titanium carbide nanopowder. J Am Ceram Soc 2009;12:2877–82.